WEMPEC

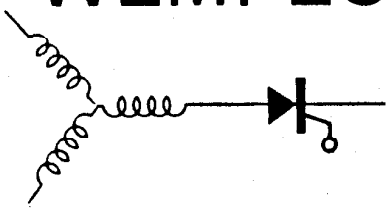

Wisconsin Electric Machines and Power Electronics Consortium

RESEARCH REPORT
82-8

Analysis and Steady-State Behavior of an Optimized AC Converter Machine

F.X. Wang and T.A. Lipo
University of Wisconsin
Madison, Wisconsin

Department of Electrical and Computer Engineering
University of Wisconsin-Madison
Madison, Wisconsin 53706

September 1982

ANALYSIS AND STEADY-STATE BEHAVIOR OF AN OPTIMIZED AC CONVERTER MACHINE

F.X. Wang and T.A. Lipo
University of Wisconsin
Madison, Wisconsin

Abstract

At present, AC machines for adjustable speed drives retain a sinusoidal winding distribution even though such machines were originally intended for sinusoidal power supplies. This paper describes a unique concentrated winding machine in which the winding distribution is intentionally rectangular to better accomodate the rectangular waveforms of conventional six pulse converters. Equations which define steady state are derived and compared with tested results on an actual prototype. Both generating and motoring modes are investigated and conditions are identified for optimal operation of this new machine.

Introduction

The continuously expanding fields of application of adjustable speed AC drives ranging from fractional to thousands of horsepower is in the process of revolutionizing the industrial drive market. This revolution, however, has not yet had a dramatic influence on the design of the associated AC drive motor. In most cases, operation from an adjustable frequency has merely influenced the careful selection of a number of conventional design constants including slot openings, rotor bar shape and skew. Designs for both synchronous and induction machines continue to be constructed using a design procedure which evolved long before the era of solid state power supplies and which is inherently based on the use of conventional constant frequency sine wave supplies rather than the harmonic rich converter supplies presently in manufacture. Recently, however, a new type of machine specifically designed for converter operation has been reported.[1] This machine is designed to develop a rectangular rather than the more conventional sinusoidal emf in order to more effectively utilize the harmonic power available from the waveform of a conventional six pulse current link and voltage link inverter. The machine consists of a stator structure having an asymmetrical six phase connection in which a pair of three phase windings have been displaced 30 electrical degrees. Each of the stator windings is comprised of concentrated full pitch windings having one slot per pole per phase. The motor employs a salient pole field structure with a pole arc of 120° (electrical) utilizing a specially designed asymmetrical pole face taper to counteract armature reaction.

At present, only the steady state experimental performance of this machine has been reported[1] and a need clearly exists to develop models which adequately predict observed transient as well as steady state behavior of this new type of machine. Because of the asymmetrical gap the inductances between stator and rotor no longer retain the sinusoidal variation characteristic of conventionally designed synchronous and induction machines. Hence the analysis of this type of machine becomes exceedingly complicated due to the fact that the usual transformations of variables, i.e. Park's and Stanley's tranformations, no longer yield a simplification in the model. In addition, practical effects such as stator and rotor slotting become more significant since stator or rotor skewing is not employed.

In this paper the first detailed analytical treatment of the concentrated winding machine is undertaken. In particular, permeance expressions are derived for all relevant inductive coupling terms within the machine. These permeance functions include the effects of slot harmonics which are shown to have an important effect on the machine behavior. The machine equations are solved by matrix analysis on a digital computer and the predicted results are shown to compare well with test. This model should permit the designer to develop new, improved versions of the CWM machine and, perhaps, make possible the practical application of such a machine.

Principle of Operation

Before modeling commences it is useful to consider how rectangular wave operation can be achieved and why such a machine is desirable when operating from a static converter supply. Consider initially, the elementary two pole machine shown in Fig. 1(a). In this machine all phases are assumed to be constructed from concentrated full pitch coils. In general, any number of phases can be selected. It can be shown that higher numbers of phases improve the performance of the machine in a manner similar to a DC machine. However, practical considerations associated with realistic converter bridge configurations limit the phase numbers to multiples of three. Figure 1 shows a winding arrangement for a six phase machine which is probably the minimum practical phase number for machines of this type. Note that with proper labeling, the six windings can be segregated into a pair of three phase groups. The groups themselves can be considered displaced by 30°.

Figure 1(a) also indicates the current through the machine at a particular time instant and can be used to illustrate how rectangular wave operation is achieved. If, for purposes of illustration, the field winding is assumed as uniformly distributed over the interpolar space, the resulting variation in field MMF around the periphery is shown by the trapezoidal solid line of Fig. 1(b). In general, if the field pole is designed in a conventional manner, that is, with a uniform gap under the pole arc, the corresponding flux density produced by this MMF would also be rectangular. This type of flux density pattern is illustrated by the dot--dashed lines in Fig. 1(b). In principle, such a waveform is precisely the variation desired if the induced air gap voltage is to quasi-rectangular. Unfortunately, the air gap voltage is proportional to the field

air gap flux only on open circuit. When the machine is subjected to armature load current the net flux becomes distorted by the resulting armature ampere turns. This difficulty may be overcome, however, if the gap along the pole is properly tapered in anticipation of the armature ampere turns which will appear on load. If the pole is tapered for generating operation such that the gap increases when moving from the front of the pole in the direction of rotation to the rear of the pole, the air gap flux produced by the field becomes distorted as shown by the dashed line in Fig. 1(b).

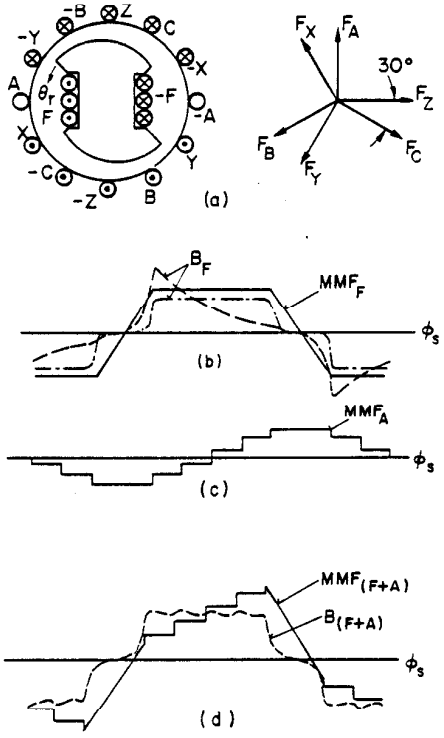

Fig. 1 (a) Winding Configuration Showing Winding Current Polarities at Particular Time Instant, (b) Flux Density and MMF Produced by Field Current, (c) MMF Produced by Armature Current, (d) Total Resultant Flux Density and MMF.

Assume now that the currents supplied to the six phases of the machine are 120° rectangular blocks such as those which flow in a current link converter bridge.[2] The triangularlike armature reaction MMF of Fig. 1(c) is then produced. The total MMF, which is equal to the spatial superposition of the field and armature MMFs, becomes the asymmetric staircase function shown in Fig. 1(d). However, if the air gap is properly designed the effects of the tapered gap and symmetric MMF cancel so that the resultant flux density in the gap becomes quasi-rectangular as also shown in Fig. 1(d). Although ripples remain due to stator slotting the air gap flux density and hence the EMF induced in each of the concentrated coils is essentially the same shape as the armature currents. Since both stator voltage and current are quasi-rectangular harmonic power as well as fundamental component of power can be considered as torque producing components. Because of the increased power obtained from the harmonics it can be shown that when such a machine feeds or draws power from a converter supply, the machine can ideally produce 15% more power output for the same copper and iron and for the same stator copper losses than with a conventional sinusoidally distributed winding construction.[1]

Mathematical Modeling of CWM Machine

It is clear that a six phase synchronous machine of any construction can always be described by a voltage differential equation of the form:

$$\mathbf{V} = \mathbf{R}\cdot\mathbf{I} + \left(\frac{1}{\omega_b}\right)\frac{d}{dt}(\mathbf{X}\cdot\mathbf{I}) \tag{1}$$

where

$$\mathbf{V} = [v_a, v_b, v_c, v_x, v_y, v_z, v_f]^T \tag{2}$$

$$\mathbf{I} = [i_a, i_b, i_c, i_x, i_y, i_z, i_f]^T \tag{3}$$

$$\mathbf{R} = \begin{bmatrix} r_a & 0 & 0 & 0 & 0 & 0 & 0 \\ 0 & r_b & 0 & 0 & 0 & 0 & 0 \\ 0 & 0 & r_c & 0 & 0 & 0 & 0 \\ 0 & 0 & 0 & r_x & 0 & 0 & 0 \\ 0 & 0 & 0 & 0 & r_y & 0 & 0 \\ 0 & 0 & 0 & 0 & 0 & r_z & 0 \\ 0 & 0 & 0 & 0 & 0 & 0 & r_f \end{bmatrix} \tag{4}$$

$$\mathbf{X} = \begin{bmatrix} x_{aa} & x_{ab} & x_{ac} & x_{ax} & x_{ay} & x_{az} & x_{af} \\ x_{ba} & x_{bb} & x_{bc} & x_{bx} & x_{by} & x_{bz} & x_{bf} \\ x_{ca} & x_{cb} & x_{cc} & x_{cx} & x_{cy} & x_{cz} & x_{cf} \\ x_{xa} & x_{xb} & x_{xc} & x_{xx} & x_{xy} & x_{xz} & x_{xf} \\ x_{ya} & x_{yb} & x_{yc} & x_{yx} & x_{yy} & x_{yz} & x_{yf} \\ x_{za} & x_{zb} & x_{zc} & x_{zx} & x_{zy} & x_{zz} & x_{zf} \\ x_{fa} & x_{fb} & x_{fc} & x_{fx} & x_{fy} & x_{fz} & x_{ff} \end{bmatrix} \tag{5}$$

The subscripts a, b, c, x, y, z correspond to the six-phase windings shown in Fig. 1(a).

The corresponding electromagnetic torque is, in general,

$$T_e = \frac{N_p}{2\omega_b}\frac{d}{d\theta_r}(\mathbf{X}\cdot\mathbf{I})^T\cdot\mathbf{I} \tag{6}$$

where ω_b is a constant selected as the base angular frequency and N_p is the number of poles.

It is apparent that the presence of an asymmetric gap introduces a formidible complication in the analysis of these equations. In general, the CWM machine possesses sufficient symmetry such that $r_a = r_b = ,..,= r_z$. In addition, conservation of energy implies that the reactance matrix X is symmetric so that $x_{ba} = x_{ab}$, etc. However, since the airgap is not symmetric the sinusoidal variation of mutual inductances inherent in the Park Transformation approach to the analysis of synchronous machines is not applicable. Nonetheless it can be shown that only seven inductances are truly independent because of the symmetrical nature of the six phase wingings, namely x_{aa}, x_{ab}, x_{ax}, x_{ay}, x_{az}, x_{af} and x_{ff}. Definition of the remaining inductances can be derived by simply phase displacing the arguments of the appropriate inductance function by 120°. The solution

for the seven inductances can be conveniently obtained by application of the theory of permeance functions.[3]

Determination of Self and Mutual Reactances

A Traditional definition of inductance parameters of conventional synchronous machines typically employs the assumptions that the airgap flux density is sinusoidal and that the stator has smooth surface. These assumptions are, however, no longer valid for the CWM machine owing to its novel construction. In order to obtain modified equations for these inductances it is useful to first concern ourselves with the airgap magnetic field.

Consider initially the case wherein only phase A is excited and that the self inductance x_{aa} is to be calculated. Neglecting the effect of saturation and curvature, a typical distribution of airgap flux density produced by current i_a is shown in Fig. 2(e). In general, the resulting airgap flux density can be thought of as composed of a product of MMF set up by the current in phase A, times an airgap permeance which depends on structure and relative position of stator and rotor. That is

$$B_g(\theta_r,\phi_s) = F_a(\phi_s)\cdot P_g(\theta_r,\phi_s) \qquad (7)$$

where $F_a(\phi_s)$ is the MMF of phase A. For a concentrated lap winding, this MMF has the rectangular waveform as shown in Fig. 2(b) having an amplitude

$$|F_a(\phi_s)| = \frac{N_{ts} i_a}{N_p N_c} \qquad (8)$$

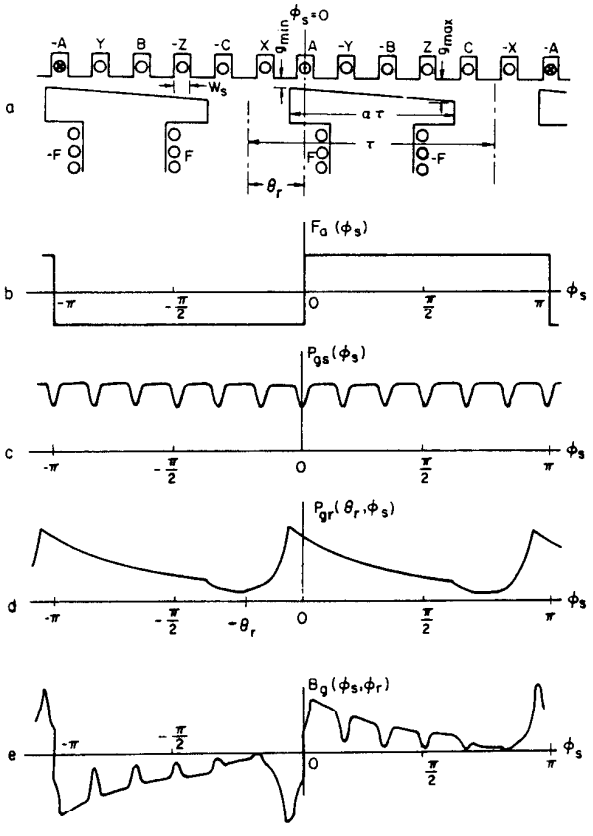

Fig. 2 (a) Rectangular Equivalent Pole Configuration Showing Winding of Phase A Excited, (b) Rectangular MMF Produced by Phase A Current, (c) Slot Shape Permeance Function, (d) Pole Shape Permeance Function, (e) Resulting Gap Flux Density Produced by Excitation.

where

N_{ts} - - - Total turns in series per phase
i_a - - - Phase current
N_p - - - Number of poles
N_c - - - Number of circuits in parallel in each phase.

It is useful to view, the airgap permeance $P_g(\theta_r, \phi_s)$ on the other hand as consisting of two components, one component concerned with the effects of the stator slot opening, and a second component which is concerned with the details of the salient pole structure. The permeance P_g can therefore be expressed as:

$$P_g(\theta_r,\phi_s) = P_{gs}(\phi_s)\cdot P_{gr}(\theta_r,\phi_s) \qquad (9)$$

where:

ϕ_s - - - Position of a particular point in the gap in the stator coordinate system. The center of slot A is taken as the origin.

θ_r - - - The relative angular rotation of the rotor coordinate origin to the stator coordinate origin as shown in Fig. 2(a).

Using the geometrical data of the computed machine the flux distribution for each excitation condition can be obtained by extending the conformal mapping techniques used for symmetrical gap machines. If the base value of $P_g(\theta_r,\theta_s)$ is taken as μ_o/g_{min} then the permeance $P_{gs}(\phi_s)$ which describes the effect of the slot opening can be expressed in per unit analytically as follows:

$$P_{gs}(\phi_s) = \begin{cases} C_{s0}\cosh\left(C_{s1}\left(\frac{\phi_s}{\pi} - \frac{K}{6}\right)\right) & \text{for } \left|\frac{\phi_s}{\pi} - \frac{K}{6}\right| < C_{sw} \\ & K = 0,1,2,\ldots,6 \\ 1.0 & \text{for } \left|\frac{\phi_s}{\pi} - \frac{K}{6}\right| > C_{sw} \\ & K = 0,1,2,\ldots,6 \end{cases} \qquad (10)$$

where the constants C_{s0}, C_{s1} and C_{sw} are defined by

$$C_{s0} = \frac{2}{\sqrt{(1+C_{g0})\left(1+\frac{1}{C_{g0}}\right)}} \qquad (11)$$

$$C_{s1} = 15.5\left(e^{0.015 w_s/g_0} - 1\right) \qquad (12)$$

$$C_{sw} = 1 + \sqrt{2}\, e^{-0.3466 w_s/g_0} \qquad (13)$$

wherein

$$C_{g0} = \left[\frac{w_s}{2g_0} + \sqrt{\left(\frac{w_s}{2g_0}\right)^2 + 1}\right]^2 \qquad (14)$$

$$g_0 = g_{min}\cdot\frac{\gamma-1}{\ln(\gamma)} \qquad (15)$$

and

$$\gamma = g_{max}/g_{min} \qquad (16)$$

In these equations g_{min} is the equivalent minimum airgap length including the increment of airgap caused by the stator slot opening (Carter's Coefficient), g_{max} is the equivalent maximum airgap length including the in-

crement of airgap caused by the stator slot opening, w_s is the stator slot opening, and μ_0 the permeability of air; $4\pi \cdot 10^{-7}$ in MKS units.

The permance $P_{gr}(\theta_r,\phi_s)$ which describes the effect of pole arc and taper can be expressed in per unit as:

$$P_{gr}(\theta_r,\phi_s) = \begin{cases} e^{-C_{r1}(\frac{1-\alpha}{2} - \frac{\theta_r+\phi_s}{\pi})} & \text{for } 0 \leqslant \frac{\theta_r+\phi_s}{\pi} < \frac{1-\alpha}{2} \\ \dfrac{1}{1+\frac{\gamma-1}{\alpha}(\frac{\theta_r+\phi_s}{\pi} - \frac{1-\alpha}{2})} & \text{for } \frac{1-\alpha}{2} \leqslant \frac{\theta_r+\phi_s}{\pi} \leqslant \frac{1+\alpha}{2} \\ \frac{1}{\gamma} e^{-C_{r2}(\frac{\theta_r+\phi_s}{\pi} - \frac{1+\alpha}{2})} & \text{for } \frac{1+\alpha}{2} < \frac{\theta_r+\phi_s}{\pi} \leqslant 1 \end{cases} \tag{17}$$

where

$$C_{r1} = 0.255\,\frac{\tau}{g_{min}} + \frac{2.776}{1-\alpha} \tag{18}$$

$$C_{r2} = 0.255\,\frac{\tau}{g_{max}} + \frac{2.776}{1-\alpha} \tag{19}$$

and τ is the pole pitch, and α is the ratio of poleshoe width to pole pitch. The waveforms of $P_{gs}(\phi_s)$ and $P_{gr}(\theta_r, \phi_s)$ are shown in Fig. 2(c) and 2(d).

Airgap flux density, airgap flux, self and mutual reactances of all windings can now be calculated by using Eqs. 7 to 19 with the appropriate arguments in Eq. 7. If current i_a flows in phase A, the self inductance of phase A can be written compactly as

$$L_{aa}(\theta_r) = \frac{\mu_0 \tau \ell}{g_{min}} \cdot \frac{N_{ts}^2}{N_p N_c} \int_0^{\pi} P_{gs}(\phi_s) \cdot P_{gr}(\theta_r,\phi_s)\,d\phi_s \tag{20}$$

where ℓ is the effective length of the core. The corresponding self reactance of phase A is

$$x_{aa}(\theta_r) = x_{am} \int_0^{\pi} P_{gs}(\phi_s) \cdot P_{gr}(\theta_r,\phi_s)\,d\phi_s \tag{21}$$

wherein

$$x_{am} = \frac{\mu_0 \tau \ell}{g_{min}} \cdot \frac{N_{ts}^2}{N_p N_c} \cdot \omega_b \tag{22}$$

is the magnetizing inductance of an equivalent smooth air gap machine having a gap g_{min}.

In the same manner the mutual reactances between the all stator windings and the field winding can also be determined. These equations are summarized as Eqs. 23-29:

$$x_{ab}(\theta_r) = x_{am}\left[\left(\int_{2\pi/3}^{\pi} - \int_0^{2\pi/3}\right) P_{gs}(\phi_s) \cdot P_{gr}(\theta_r,\phi_s)\,d\phi_s\right] \tag{23}$$

$$x_{ac}(\theta_r) = x_{am}\left[\left(\int_0^{\pi/3} - \int_{\pi/3}^{\pi}\right) P_{gs}(\phi_s) \cdot P_{gr}(\theta_r,\phi_s)\,d\phi_s\right] \tag{24}$$

$$x_{ax}(\theta_r) = x_{am}\left[\left(\int_{\pi/6}^{\pi} - \int_0^{\pi/6}\right) P_{gs}(\phi_s) \cdot P_{gr}(\theta_r,\phi_s)\,d\phi_s\right] \tag{25}$$

$$x_{ay}(\theta_r) = x_{am}\left[\left(\int_0^{5\pi/6} - \int_{5\pi/6}^{\pi}\right) P_{gs}(\phi_s) \cdot P_{gr}(\theta_r,\phi_s)\,d\phi_s\right] \tag{26}$$

$$x_{az}(\theta_r) = x_{am}\left[\left(\int_0^{\pi/2} - \int_{\pi/2}^{\pi}\right) P_{gs}(\phi_s) \cdot P_{gr}(\theta_r,\phi_s)\,d\phi_s\right] \tag{27}$$

$$x_{af}(\theta_r) = x_{am} \frac{N_{tf}}{N_{ts}} \left[\left(\int_0^{\pi-\theta_r} - \int_{\pi-\theta_r}^{\pi}\right) P_{gs}(\phi_s) \cdot P_{gr}(\theta_r,\phi_s)\,d\phi_s\right] \tag{28}$$

$$x_{ff}(\theta_r) = \frac{\mu_0 \tau \ell}{g_{min}} \cdot \frac{N_{tf}^2}{N_p}\, \omega_b \int_{-\theta_r}^{\pi-\theta_r} P_{gs}(\phi_s) \cdot P_{gr}(\theta_r,\phi_s)\,d\phi_s \tag{29}$$

In Eqs. 28 and 29 N_{tf} is the total series connected turns in the field winding. Note that in each case an integral over one pole pitch is taken. The integrals which express mutual reactance have been explictly broken into two portions in order to indicate the manner in which each integral must be evaluated.

Experimental Determination of Reactances

Although the calculation of the machine self and mutual reactances are formidible, the corresponding measurement on an experimental prototype is fortunately less difficult. A simple, direct approach is to carry out a stationary test in which the rotor is locked and one phase, say phase A, is supplied with AC current while all the other windings remain open circuited. The current in phase A and voltages of all windings are then measured for each specified rotor position.

The total self reactance including the leakage reactance of phase A is, for example:

$$x_{aa}(\theta_r) = \sqrt{\left(\frac{V_{aa}(\theta_r)}{I_a(\theta_r)}\right)^2 - r_a^2} \tag{30}$$

where $V_{aa}(\theta_r)$ and $I_a(\theta_r)$ are the RMS values of voltage and current of phase A for each specified rotor position θ_r, and r_a is the resistance of phase A.

The mutual reactances can be determined in like manner. For instance, the mutual reactance between phases A and B is

$$x_{ab}(\theta_r) = \frac{V_{ab}(\theta_r)}{I_a(\theta_r)} \tag{31}$$

where $V_{ab}(\theta_r)$ is the open circuit voltage measured at phase B for the specified value of θ_r.

In order to carry out the solution of the machine system voltage equation, Eq. 1, the time or, equivalently, the spatial derivatives of all reactance coefficients must also be determined. One possible means of measuring these quantities is by taking derivatives of the measured reactance values. However, this method is not sufficiently accurate due to the unavoidable measurement error. Fortunately it is possble to measure these derivative terms directly. In this case the tested machine is driven by a DC motor and one phase, for example phase A, is supplied with a DC current. All other windings remain open circuited. The voltage waveform of each winding can now be recorded with an oscilloscope. Since the current is constant, the voltages observed are proportional to the time rate of change of inductance terms in Eq. 1. An important requirement in this test is that pure DC current must be maintained by insertion of a large inductor in phase A, otherwise substantial error can be produced.

In order to verify the accuracy of the design equations which have been developed a prototype 10 HP synchronous machine has been designed and built. The self and mutual reactances and their derivatives for this machine were both calculated and measured. The results are shown in Figs. 3 to 8. The comparison clearly shows that the calculated values are very close to the tested results and that even the slot ripple harmonics are reproduced with relatively good accuracy. It is apparent from these curves that the reactances of CWM machine are quite different from a conventional

synchronous machine. Clearly the inductances are not sinusoidal functions of rotor position nor are they symmetric about the d and q axis.

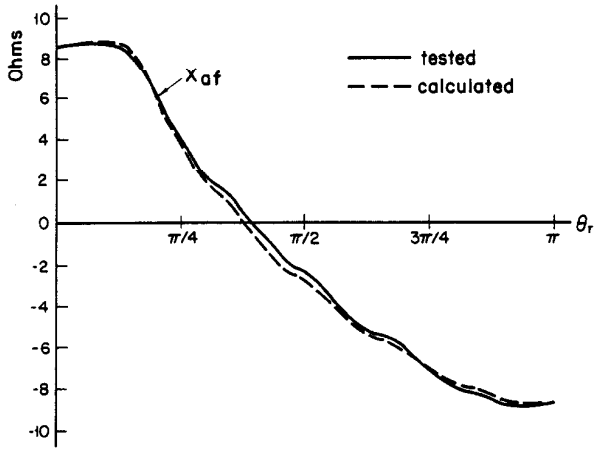

Fig. 3 Comparison of Tested and Calculated Values of Mutual Reactance x_{af} as a Function of Rotor Position.

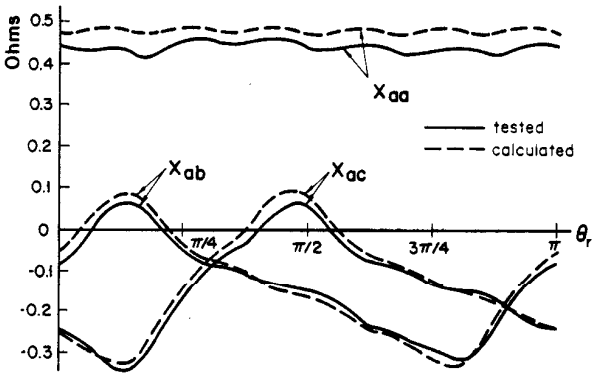

Fig. 4 Tested and Calculated Variation of Reactances x_{aa}, x_{ab}, and x_{ac} as a Function of Rotor Angular Position θ_r.

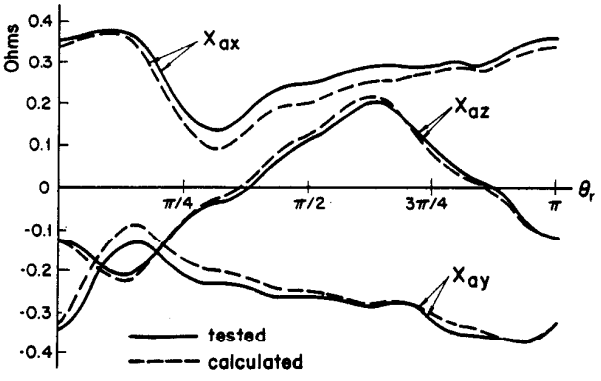

Fig. 5 Comparison of Tested and Computed Variation of Reactances x_{ax}, x_{ay}, and x_{az} as a Function of Rotor Position.

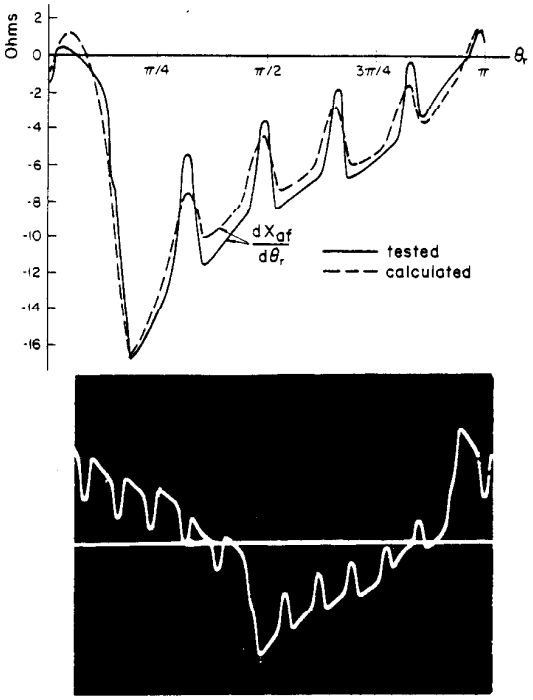

Fig. 6 Comparison of Computed and Tested Values of Speed Voltage Coefficient $dx_{af}/d\theta_r$.

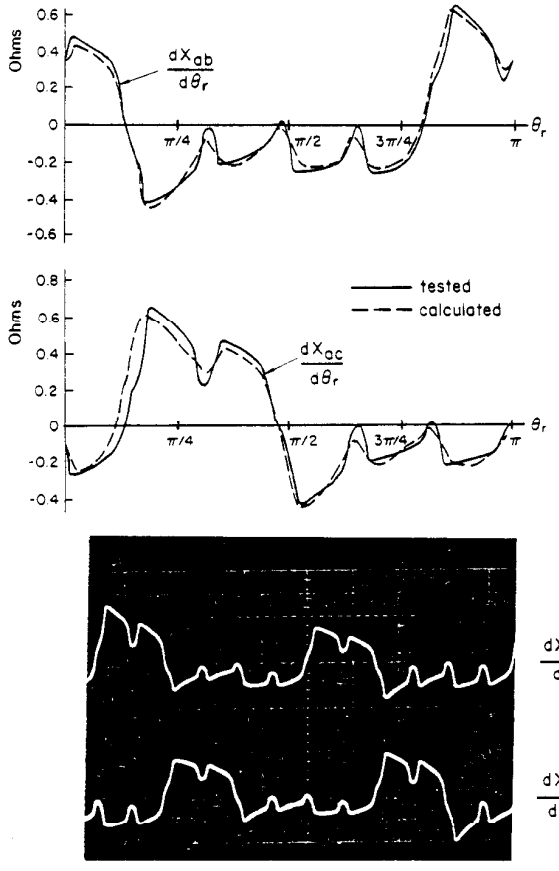

Fig. 7 Comparison of Computed and Measured Traces of the Speed Voltage Coefficients $dx_{ac}/d\theta_r$ and $dx_{ab}/d\theta_r$.

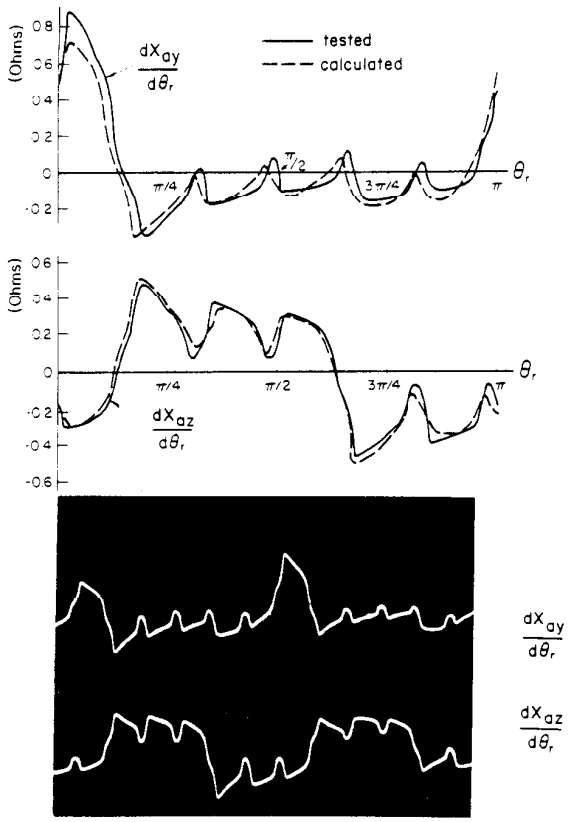

Fig. 8 Comparison of Computed Waveforms and Measured Traces of Speed Voltage Coefficients $dx_{ay}/d\theta_r$ and $dx_{az}/d\theta_r$.

Analysis of Generating Mode

Although opportunities for the CWM machine exist with a motor, this machine can also operate as a synchronous generator with quasi-rectangular waveform. Application possibilities also exist in the generating mode. Specifically, an extensive study was conducted to evaluate the feasibility of constructing a low ripple DC supply as shown in Fig. 9. It is interesting to note that because of the inherent rectangular waveshape produced by the machine a smooth DC current inherently flows and, therefore, a DC link filter inductor is not necessarily required.[1]

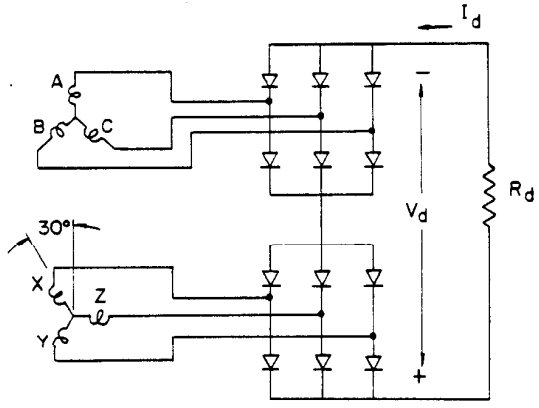

Fig. 9 Circuit Illustrating CWM Machine Operating as a Generator Feeding a Diode Bridge-Resistive Load.

A typical voltage waveform for the connection of Fig. 9 is given in Fig. 10 for the following operating condition:

Rotor Speed	ω_r = 900 RPM
Field Current	I_f = 8.4 Amps
DC Load Current	I_d = 14.0 Amps (Pure Resistance Load).

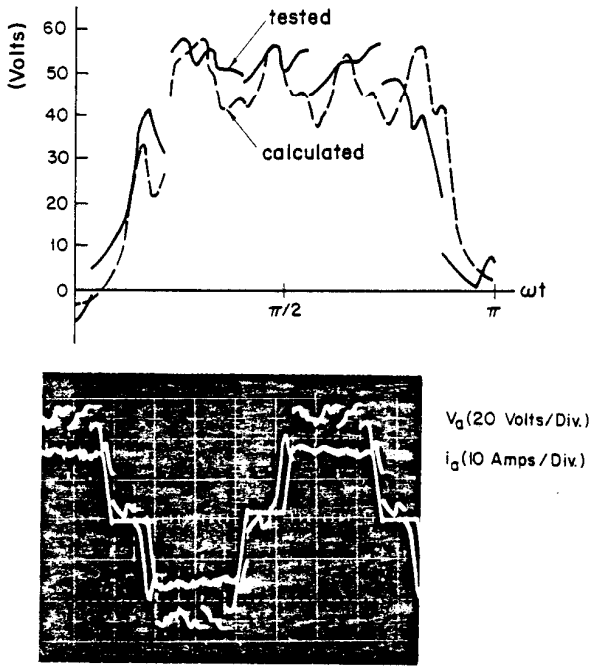

Fig. 10 Comparison of Calculated and Measured Phase to Neutral Voltage.

The solid line shows the results obtained from test while the dashed line is the result of a computer solution of Eq. 1. It is evident that even with modern computational tools the evaluation of Eq. 1 is formidible. However, if the currents are known, the voltage waveforms can be calculated by substituting the calculated parameters into Eqs. 1 to 5. It is apparent that the computation of terminal voltage from current is much easier and more straightforward than the reverse alternative.

It is useful to consider the individual terms which appear in Eq. 1 in more detail. In particular, the voltage of phase A can be solved from the first row of Eq. (1), that is:

$$v_a = \frac{\omega_r}{\omega_b}\frac{dx_{af}}{d\theta_r} i_f + \frac{1}{\omega_b} x_{af}\frac{di_f}{dt} + \frac{\omega_r}{\omega_b}\sum_{\substack{k=a,b,c\\x,y,z}}\frac{dx_{ak}}{d\theta_r} i_k + \frac{1}{\omega_b}\sum_{\substack{k=a,b,c\\x,y,z}} x_{ak}\frac{di_k}{dt} + r_a i_a \quad (32)$$

where $\omega_r = d\theta_r/dt$ is the rotor angular frequency.

From examination of Eq. 32 it can be observed that the phase voltage consists of five different components each of which are plotted in Fig. 11. These terms are namely:

1) $\frac{\omega_r}{\omega_b} \cdot \frac{dx_{af}}{d\theta_r} i_f$

This component is the speed EMF produced by the time rate of change of x_{af} during rotation.

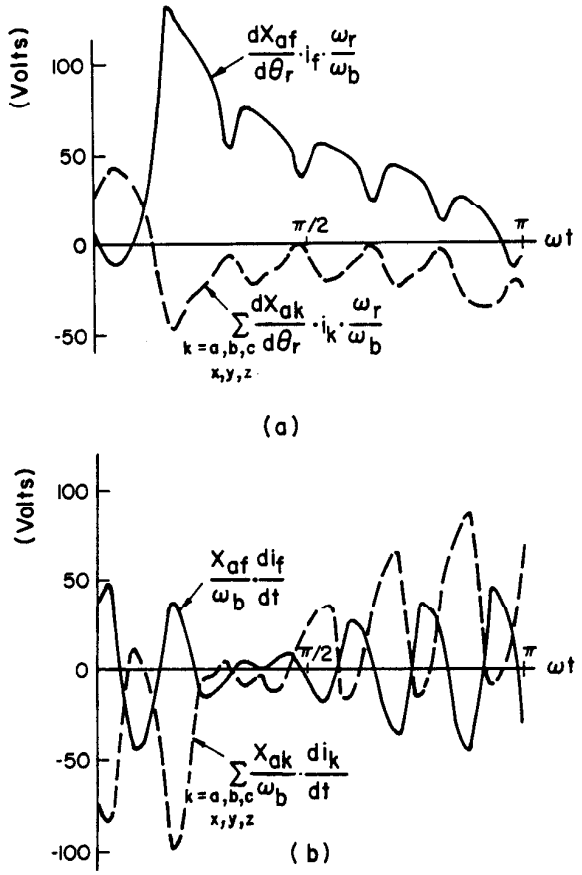

Fig. 11 Illustrating Contributions of Individual Terms to Phase to Neutral Voltage of Fig. 10.

2) $\frac{1}{\omega_b} x_{af} \frac{di_f}{dt}$

This term might be called transformer EMF due to the variation of field current. For a conventional synchronous machine this term is small and usually can be neglected. For the CWM machine, however, its value could be significant as seen from Fig. 11. Because of the special structure of winding and pole, the field current will clearly contain a greater portion of MMF and permeance harmonics resulting in time harmonics in the field current.

3) $\frac{\omega_r}{\omega_b} \sum_{\substack{k=a,b,c \\ x,y,z}} \frac{dx_{ak}}{d\theta_r} i_k$

These components are the speed induced EMF of armature reaction produced by the time rate of change of self and mutual reactances during rotation.

4) $\frac{1}{\omega_b} \sum_{\substack{k=a,b,c \\ x,y,z}} x_{ak} \cdot \frac{di_k}{dt}$

The terms given by 4) are the transformer EMF of armature reaction due to the time variation of the phase currents. It should be mentioned that because the armature currents have a quasi-rectangular waveform, the derivatives di_k/dt could become a very large value and produce a large commutation EMF pulse. The presence of these terms appears to explain why spikes appear in the voltage waveform as seen in Fig. 10.

5) $r_a \cdot i_a$

This quantity represents the resistive voltage drop. Its value is small in comparison to the other components.

One interesting observation from Fig. 11 is the fact that the term $(\omega_r/\omega_b)\sum(dx_{ak}/d\theta_r)i_k$ has a waveform similar to $(\omega_r/\omega_b)(dx_{af}/d\theta_r)i_f$ except with an opposite sign. The terms $(1/\omega_b)\sum x_{ak}(di_k/dt)$ and $(1/\omega_b)x_{af}(di_f/dt)$ have nearly an equal but opposite relationship as does the terms $(\omega_r/\omega_b)\sum(dx_{ak}/d\theta_r)i_k$ and $(\omega_r/\omega_b)(dx_{af}/d\theta_r)i_f$, as shown in Fig. 11. This behavior is simply a manifestation of armature reaction since field and armature windings of inductive circuits will always tend to oppose each other.

It is clear that maintaining a rectangular voltage waveform is not a simple matter since the terminal voltage consists of 15 terms and is affected by many factors. For a machine with fixed parameters, performance will depend on the armature currents (both amplitude and phase angle), field current and rotor speed. In addition, geometrical design factors such as winding structure, pole shape, airgap length, stator slot opening etc., clearly will affect the voltage and current waveform.

Electromagnetic Torque

Having obtained the machine voltages and currents, the instantaneous and average torque can be calculated readily from Eq. 6. However, it is well known that it is difficult to measure instantaneous torque of any machine directly. Fortunately, its value can be determined indirectly. Neglecting the stator losses, the instantaneous torque approximately equals the output power divided by the mechanical speed ω_{rm}, i.e.

$$T_e = \frac{i_d^2 r_d}{\omega_{rm}} \tag{33}$$

where:

i_d --- Instantaneous Load Current
r_d --- Load Resistance
ω_{rm} -- Rotor Mechanical Angular Frequency

Because only relatively high frequency torque harmonics appear, (sixth harmonic and its multiples) the mechanical speed can be considered as a constant over one cycle. Since the DC load current i_d can be recorded by oscilloscope, the instantaneous torque can therefore be determined directly from the measured i_d waveform. If the average torque measured directly from a dynamometer is taken as the base value the instantaneous per unit torque obtained analytically from Eq. 6 and from test by Eq. 33 are shown in Fig. 12. A relatively small amount of pulsating torque equal to about 1/9 that of a machine of conventional design is observed.[1,4] A substantial reduction in both harmonic power flow at the DC link as well as in harmonic components of electromagnetic torque is clearly a major advantage of the CWM machine.

Condition for Optimal Operation

The optimal operation of any machine is typically the case which gives maximum efficiency. For the CWM machine, the condition of the optimal operation corresponds to the condition in which a rectangular waveform

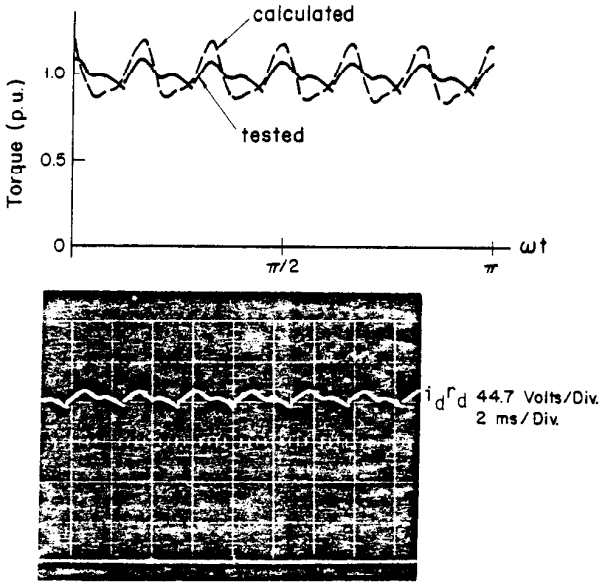

Fig. 12 Comparison of Computed Electromagnetic Torque with Calculated Results from Test. CWM Machine Feeding Diode Bridge Load of Fig. 9.

is maintained for both voltage and current. In general, four variables can affect the operating condition of the CWM machine, namely field current I_f, load current I_d, property of the load (i.e. the power factor PF) and the rotor speed ω_r. Under the optimal operation the relationship between these variables must be as follows:

a) When I_f, I_d and PF are constant, the change of rotor speed does not affect the voltage and current waveform. This conclusion is verified by reference to Fig. 14. Moreover, the average torque is almost constant when the rotor speed changes. Hence the CWM machine has desirable constant torque characteristics as shown in Fig. 13.

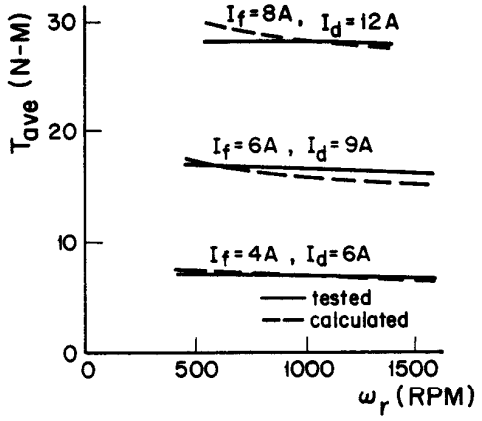

Fig. 13 Average Torque Variation with Rotor Speed for Various Values of Field and Load Current.

b) In order to keep the same rectangular waveform, the field current I_f must be adjusted when the load current I_d changes. Within the nonsaturation region I_f should be maintained proportional to I_d. A measured characteristic indicating a slight effect of saturation is shown in Fig. 15.

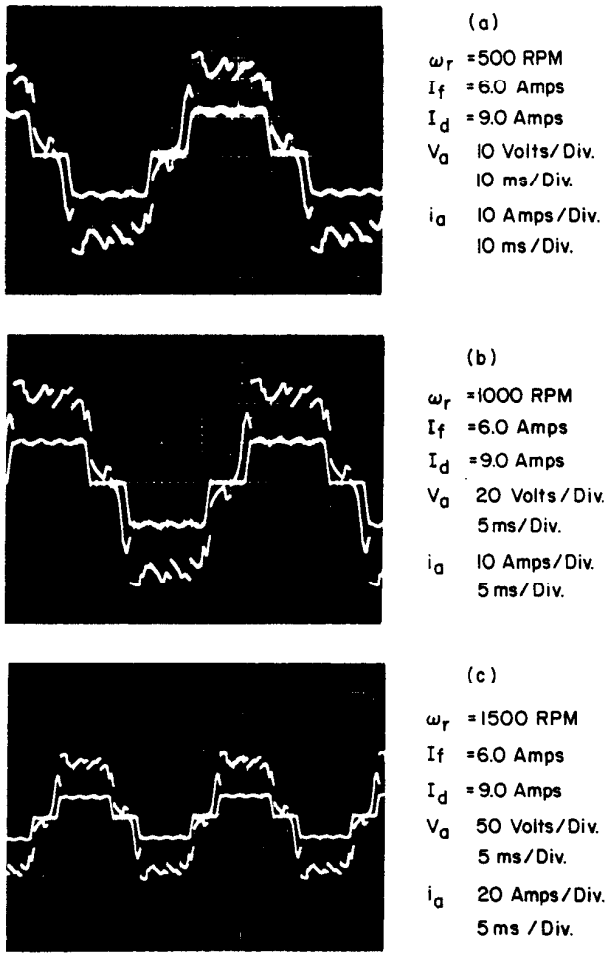

Fig. 14 Phase Voltage and Current of CWM Machine Connected to a Diode Bridge Load as Rotor Speed Changes.

c) If rectangular waveform is maintained the average torque is independent of ω_r, and is almost proportional to the square of load current I_d or field current I_f, as shown in Fig. 16. Hence, for a fixed resistance load, the average torque is proportional to output power.

d) The CWM generator appears to prefer a resistive load and it is more difficult to maintain a rectangular voltage and current waveform for an inductive or capacitive load.

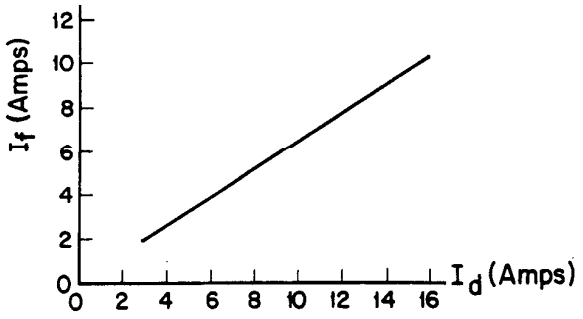

Fig. 15 Optimal Variation of Field Current as a Function of Armature Currrent to Maintain Rectangular Waveform.

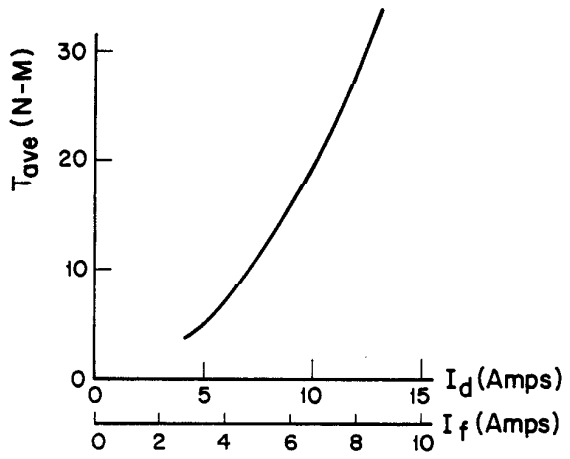

Fig. 16 Variation of Average Torque when I_f and I_a are Adjusted Under the Optimum Conditions Required to Maintain Rectangular Voltage and Current Waveform.

Investigation of Motoring Mode

It is apparent that, like any machine, a CWM machine can operate in the motoring mode. The primary problem relates to what kind of inverter is more suitable for driving such a machine. It appears that the conventional six step VSI type inverter is not suitable as a supply for variable speed operation since the required current waveform would be difficult to control. The six step CSI has the potential for being better suited than a VSI inverter since the current waveform is shaped inherently to 120° blocks. Fig. 17 gives the measured and calculated waveforms for the following case:

ABC Windings Supplied with 3 Phase CSI
Other Windings (X,Y,Z) Open Circuited
I_d = 5.0 Amps
ω_r = 900 RPM.

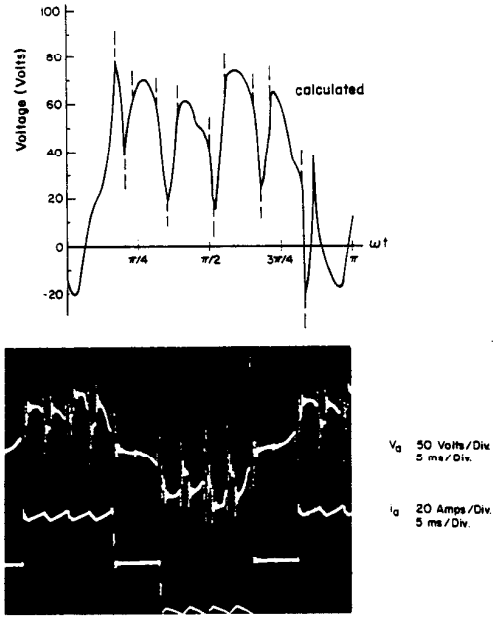

Fig. 17 Comparison of Theory with Test Result for CWM Machine Operating as a Motor Driven from a Three Phase Current Source Inverter.

Note that excellent correlation with test is again obtained suggesting that the analysis techniques developed in this paper are equally valid for the motoring mode. It can be noted that large spikes appear in the voltage waveform because of the rapid change in phase currents which occur during commutation. This problem clearly arises from the absence of amortisseur windings which was intentionally omitted from the design. The influence of a short circuited rotor cage on the performance of a CWM machine is a topic for future study. The presence of large commutating spikes is clearly detrimental to satisfactory behavior. However, from the analysis of the generating mode it appears that a six phase CSI connection may provide improved performance.

As an alternative to CSI inverter operation it appears to be practical to utilize a PWM inverter to drive the CWM motor. In this case the PWM current can be modulated in a quasi-rectangular waveform. The amplitude of the "commutation spikes", which would in this case be simply portions of the PWM waveform, could be controlled by adjusting the DC link voltage. An investigation of this type of motor drive system is presently underway.

Conclusion

This paper has set forth the first analytical treatment of the analysis of a unique new concentrated winding machine specifically designed for operation from a converter supply. Equations for the computation of all machine inductances have been derived and have been correlated satisfactorily with test. Terminal voltages and electromagnetic torque have been computed using the design equations and have been to correlate well with test. Operation of the CWM machine as both a generator and a motor has been investigated. Optimal operation of CWM machine has been discussed and the manner to keep the rectangular waveforms of voltage and current identified. Under the optimal operation, it has been shown that the average torque is independent of rotor speed and is proportional to the square of load current or field current. Maintenance of the rectangular waveform requires a linear variation of field current with the load. Operation of the CWM machine as a motor has been investigated using a three phase CSI inverter. Result indicate the need for a special six phase inverter for satisfactory operation. An investigation to find a more suitable inverter supply for motoring operation is underway.

Acknowledgement

Mr. F.X. Wang is a Visiting Scholar from the People's Republic of China. The authors wish to thank the General Electric Company for help in constructing the prototype machine, particularly to W.R. Oney and R. Keys who were responsible for fabricating the rotor and stator of the machine respectively. The work reported in this paper was partially sponsored by the industrial members of WEMPEC, the Wisconsin Electric Machines and Power Electronics Consortium.

References

1. T.A. Lipo and F.X. Wang,"Design and Performance of a Converter Optimized AC Machine". IEEE-IAS Annual Meeting Conference Record, Oct. 4-7, 1982, San Francisco CA, (to appear).
2. E.W. Kimbark,"Direct Current Transmission". J. Wiley & Sons Inc., New York NY, 1971 (book).
3 M. Liwschitz-Garik and C.C. Whipple,"AC Machines", 2nd. Ed., D. Van Nostrand Co. Inc., Princeton NJ, 1961 (book).
4. R. L. Steigerwald and T.A. Lipo,"Analysis of a Novel Forced-Commutation Starting Scheme for a Load Commutated Synchronous Motor Drive". IEEE Trans. on Ind. Appl., Vol IA-15, Jan/Feb 1979, pp. 14-24.